Available online at www.sciencedirect.com
SCIENCE DIRECT®
Journal of Catalysis 225 (2004) 213–222
JOURNAL OF CATALYSIS
www.elsevier.com/locate/jcat

Ni-exchanged AlMCM-41—An efficient bifunctional catalyst for ethylene oligomerization

Vasile Hulea * and François Fajula

Laboratoire de Matériaux Catalytiques et Catalyse en Chimie Organique, UMR 5618 ENSCM CNRS, 8 rue de l'Ecole Normale,
34 216 Montpellier cedex 5, France

Received 3 February 2004; revised 13 April 2004; accepted 15 April 2004

Abstract

A series of Ni-exchanged AlMCM-41 catalysts with carefully controlled concentrations of metallic and acidic sites was prepared, characterized, and tested in ethylene oligomerization performed in slurry batch mode. The mesoporous materials were characterized using various techniques including X-ray diffraction, nitrogen sorption measurements, temperature-programmed desorption of NH_3, thermal gravimetric analysis, and temperature-programmed reduction. The presence of a uniform pore-size distribution in the ordered mesoporous materials is very favorable for the oligomerization process. High activities were obtained for most of tested catalysts, and the reaction was highly selective, resulting almost exclusively in olefins with an even number of C_4–C_{12} carbon atoms. Both metal and acid sites are required for the activation of ethylene oligomerization. However, the samples with lower acidity showed very high reaction activity and stability due to their lower deactivation rate. The catalytic activity and product spectrum showed a pronounced dependence on the oligomerization conditions. Thus, the ethylene conversion goes through a maximum at 150 °C reaction temperature, and increased linearly when the pressure increased from 2 to 5 MPa. *n*-Heptane was found to be an efficient solvent for the ethylene oligomerization.

Keywords: Nickel; Ni–AlMCM-41; Ethylene; Oligomerization; Acidity

1. Introduction

The oligomerization of ethylene is of considerable academic and industrial interest for the synthesis of higher olefins, which are valuable products used in the manufacture of detergents, plasticizers, oil additives, fatty acids, etc. Moreover, as a consequence of environmental concerns, there is an increasing interest in the production of aromatics and sulfur-free transportation fuels via lower olefins oligomerization.

The neutral Ni complexes are the most widely used as homogeneous catalysts for industrial ethylene oligomerization due to their high activity and capability to direct the reaction toward specific target products [1]. Other usual homogeneous catalysts are AlR_3 (Ziegler type) and $Me(OR)_4$–AlR_3 (Ziegler–Natta type) [1].

A significant research effort has also been directed to the development of a heterogeneous process to take advantage of easy separation of catalyst and oligomers [2–19]. Nickel-loaded zeolites [2–7], usually obtained by metal ion exchange showed good catalytic activity in the gas-phase reaction of ethylene.

Unfortunately, most of these catalysts suffered a severe deactivation during the oligomerization reaction, mainly due to the blocking of micropores with heavy products [5–7]. It was found that the strong acid sites are responsible for the formation of those products by further transformations of primary oligomers. One of the approaches to overcome these problems was the use of a catalyst with larger pores and tuneable acidity, under mild oligomerization conditions. It was reported that in a three-phase slurry reactor, at low temperature, the nickel/sulfated-alumina [9,10] and especially Ni-exchanged amorphous silica–alumina (NiSA) [11] catalysts are active and very stable for the ethylene oligomerization. Thus, the rate of ethylene oligomerization (120 °C, 3.5 MPa) obtained with NiSA (1.56 wt% Ni, 425 m^2/g BET surface area) was 11.5 $g/(g_{cat}\,h)$.

---

[*] Corresponding author. Fax: +33 4 67 16 34 70.
E-mail address: hulea@cit.enscm.fr (V. Hulea).

0021-9517/$ – see front matter © 2004 Elsevier Inc. All rights reserved.
doi:10.1016/j.jcat.2004.04.018

In this context, it appeared very appealing to test in ethylene oligomerization nickel catalysts based on well-structured MCM-41 mesoporous materials. These materials have certain advantages over their microporous counterparts, viz., highly ordered mesoporosity, large surface area and pore volume, and moderate acidity [20]. The concentration and the strength of acid sites may be tuned by the incorporation of different amounts of Al atoms into the MCM-41 framework. Moreover, MCM-41-type materials can be modified by several techniques such as ion exchange, adsorption, and grafting to generate new acid, base, and redox active sites.

In a previous report, Hartmann et al. [21] have shown that Ni-MCM-41 and Ni–AlMCM-41 are catalytically active for ethylene dimerization (after a 24-h reaction period, in a static gas-phase reactor the ethylene conversion was near 5%). To our knowledge, no detailed investigation using Ni-containing mesoporous materials as catalyst for ethene oligomerization has been performed. Here we report a comprehensive study on C_2H_4 oligomerization over Ni–AlMCM-41. In order to understand the influence of nickel ion and acid sites on the catalytic performance, a series of Ni ion-exchanged mesoporous silica–aluminas with a carefully controlled concentration of Ni^{2+} and acidic sites was prepared and characterized. Our attention has also been focused on the effect of reaction conditions on the ethylene oligomerization performed in slurry batch mode.

2. Experimental

2.1. Preparation of catalysts

Al-MCM-41 materials (MSA) with varying Si/Al ratios were synthesized by autoclaving gels with a molar composition of: Al_2O_3:x SiO_2:2.5 Na_2O:CTABr:500 H_2O (x varies with Si/Al ratio). In a typical synthesis, 5 g of NaOH (Carlo Erba), y g of $NaAlO_2$ (Carlo Erba), 18.22 g of CTABr (Aldrich), and 30 g of SiO_2 (Aerosil 220 V, Degussa) were successively added under vigorous agitation to 225 g of distilled water ($y = 4.1$, 2.05, 1.37, 0.82, and 0.51 for Si/Al gel ratios of 10, 20, 30, 50, and 80, respectively). The resulting gel was stirred for 1 h at room temperature and then was autoclaved for 24 h at 130 °C. The solid was separated from the solution by filtration, washed thoroughly with deionized water, and dried at 80 °C for 12 h. The sample was finally calcined at 550 °C in air for 8 h to expel the template. A larger pore-size MSA sample was synthesized by using trimethylbenzene as a swelling agent, according to previously published procedure [22].

The as-synthesis Na^+-mesoporous silica–alumina sample (Na-MSA) was converted into NH_4^+ form (NH_4-MSA) by cationic exchange with ammonium nitrate. Thus, 5 g of Na-MSA was contacted three times at 40 °C for 2 h, under constant agitation (600 rpm), with 200 cm^3 of 0.1 M alcoholic solution of NH_4NO_3. The solid was then separated by filtration, washed with deionized water, and dried at 80 °C for 12 h. The NH_4-MSA was subjected to nickel-ion exchange with a 0.1 M alcoholic solution of nickel nitrate, following the same procedure as above. The resulting Ni–NH_4-MSA sample was finally calcined for 5 h at 550 °C to obtain the H form, denoted in this study Ni-MSA.

2.2. Characterization of catalysts

The phase identification of the calcined samples was carried out by XRD, using Cu-K_α radiation. The samples were scanned from 0.5° to 7° (2θ) angle in steps of 0.5°. The textural characterization was achieved using a conventional gas adsorption method. N_2 adsorption/desorption isotherms were measured with a Micrometrics ASAP 2000 automatic analyzer at 77 K. Specific surface areas were calculated by the BET method, the mesopore volume was determined by nitrogen adsorption at the end of capillary condensation, and pore size distribution was determined from the desorption isotherms.

The samples acidity was measured by temperature-programmed desorption (TPD) using ammonia as probe. Prior to TPD experiments, the solids were pretreated in air flow at 450 °C for 5 h. Ammonia was adsorbed for 15 min at 100 °C. The physisorbed ammonia was removed by evacuation of sample at 100 °C for 4 h, in a dry nitrogen stream. The ammonia desorption was carried out in nitrogen stream at a heating rate of 10 °C/min up to 650 °C. The amount of desorbed ammonia was monitored with a conductivity cell.

The state of the nickel species in the prepared catalysts was established by temperature-programmed reduction (TPR), using a Micromeritics AutoChem 2910 apparatus. Prior to TPR, 140 mg of sample placed in a quartz tube reactor was treated at 1000 °C in air for 1 h. The TPR was carried out using H_2/He (25/75, v/v) at a flow rate of 13 cm^3/min. The temperature was increased linearly from 25 to 1000 °C at a heating rate of 10 °C/min. The hydrogen consumption was monitored with a thermal conductivity detector.

Thermogravimetric-differential thermal analysis (TG-DTA) was carried out in a Netzsch TG 209C thermobalance. About 15 mg of catalyst was loaded, and the airflow used was 50 cm^3/min. The heating rate was 20 °C/min and the final temperature was 850 °C.

2.3. Oligomerization procedure

The catalytic ethylene oligomerization was performed in a 0.3 l well-mixed gas-slurry reactor operating in batch mode. Prior to each experiment, the catalyst was pretreated in autoclave at 150 °C for 15 h under atmospheric pressure nitrogen flow. The autoclave was then cooled at 80 °C and charged with 100 ml of dry oxygen-free organic solvent. The reactor was heated to the desired temperature under constant agitation (800 rpm) and the pressure was raised to the operating level by ethene feeding. During the experiment ethylene was continuously fed so that the total pressure was maintained constant in the reactor.

After the reaction, the autoclave was cooled in ice water, and then the liquid products were collected, weighted, and analyzed. Analysis of oligomers was performed by GC on a HP 5890 chromatograph, equipped with a flame ionisation detector and a DB-1 60 m capillary column. The following temperature program of the oven was adopted: 40 °C for 3 min, after which the temperature was increased by 10 °C/min heating rate until 250 °C was reached. In this way, it was possible to separate the olefins of C_4–C_{16} cuts.

3. Results and discussion

3.1. Characterization of catalysts

MSA samples were amorphous mesoporous materials with XRD pattern of MCM-41 type. Both XRD and N_2 sorption measurements showed that this structure was preserved during the nickel exchange. The main properties and the concentration of acid sites of some parent mesoporous materials and NiMSA*n* samples (*n* is the molar Si/Al ratio in gel synthesis) are given in Table 1. It is evident that both surface area and pore volume decreased with increasing Al content, but the effect of the Si/Al ratio on pore diameter is less important. The textural properties of MSA materials were completely preserved during Ni exchange.

MSA and NiMSA materials displayed nitrogen adsorption/desorption isotherms of type IV according to the IUPAC nomenclature [23]. As can be seen in Fig. 1 no hysteresis was obtained in the case of N_2 isotherms of catalyst having pore sizes less than 40 Å. For this sample, the sharp inflection at p/p^0 of about 0.35 indicates a uniform mesopore system. NiMSA30 ($d = 86$ Å) exhibits an irreversible type IV adsorption/desorption isotherm with a H1 hysteresis loop at $p/p^0 = 0.75$. The BJH model pore-size distribution indicates a narrow size distribution.

The acidic properties of the NiMSA samples were investigated by means of NH_3-TPD, a technique which provides general information about the number and distribution of the acid sites. As expected, the concentration of the accessible acid sites decreases as the Si/Al ratio increases (Table 1). Thus, increasing the Si/Al ratio from 10 to 80 led to a considerable decrease in acidity (from 0.72 to 0.27 mmol/g). We consider that for our NiMSA samples (having a relatively close nickel content, Table 1) the amount of acid sites was mainly affected by the Si/Al ratio and less by the degree of nickel ion exchange.

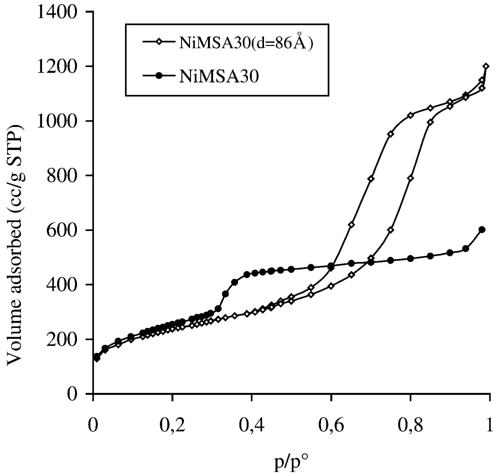

Fig. 1. N_2 isotherms of NiMSA30 and NiMSA30 ($d = 86$ Å).

Ammonia TPD profiles of NiMSA materials with different Si/Al ratios are plotted in Fig. 2. For all catalysts there is a large ammonia desorption band between 200 and 450 °C with a maximum intensity at about 250 °C. This TPD profile suggests that the NiMSA catalysts have mainly weak and medium acid sites.

Ammonia TPD measurements have also evidenced that the acidic properties of MSA materials changed during the ion exchange of NH_4^+ with Ni^{2+}. On the one hand, the quantitative evaluation of acidity (Table 1, entries 1, 2, 5, and 6) indicates that the total number of acid sites in the NiMSA is higher than for the MSA support. On the other hand, NiMSA samples show a higher density of weak and

Table 1
Physicochemical properties of MSA and Ni-containing MSA catalysts

Entry	Material	Molar Si/Al ratios		Ni	BET surface	V_{meso}	Mesopore	Acidity
		Gel	Solid[a]	(wt%)	area (m^2/g)	(ml/g)	diameter[b] (Å)	(mmol/g)
1	HMSA30[c]	30	26.5	–	945	0.70	37	0.40
2	HMSA50[c]	50	49.0	–	950	0.72	39	0.26
3	NiMSA10	10	10.2	0.6	825	0.53	34.5	0.72
4	NiMSA20	20	18.2	0.5	930	0.68	36.5	0.59
5	NiMSA30	30	26.2	0.5	940	0.70	37	0.45
6	NiMSA50	50	49.1	0.4	950	0.72	39	0.34
7	NiMSA80	80	75.4	0.3	975	0.75	39	0.27
8	NiMSA30 ($d = 86$ Å)[d]	30	25.7	0.5	830	1.53	86	0.45

[a] Determined by ICP measurements.
[b] De Boer (desorption).
[c] Obtained from NH_4-MSA (450 °C, 5 h).
[d] Synthesized with TMB as a swelling agent.

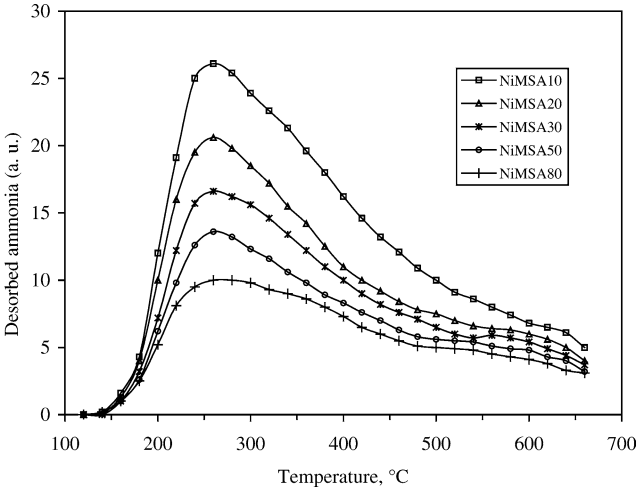

Fig. 2. TPD profiles of NiMSA catalysts.

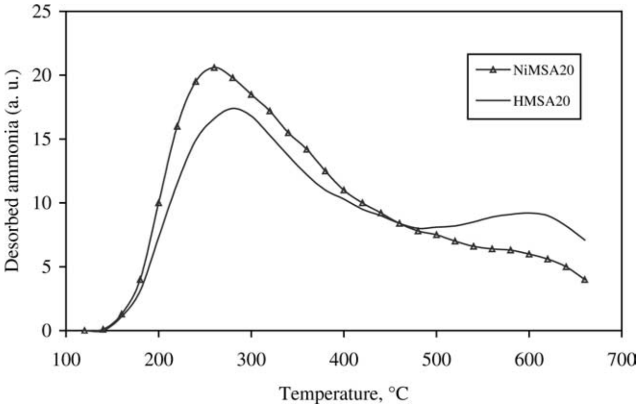

Fig. 3. TPD profiles of NiMSA20 and HMSA20 catalysts.

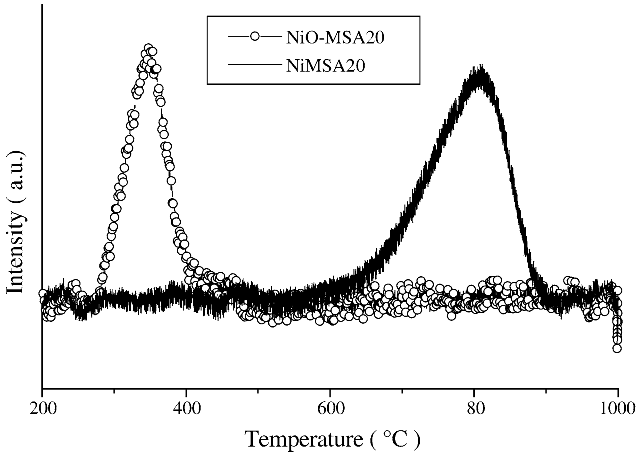

Fig. 4. TPR profile of NiMSA20 and NiO-MSA20.

medium acid sites and a lower density of strong acid sites compared to HMSA sample (Fig. 3). In fact, during the ion exchange, the original strong Brønsted acid sites were substituted by Ni cations and a new weaker acidity was generated by the metal sites.

This type of acid sites was already observed in the case of other Ni-containing molecular sieves. Minchev et al. [24] suggested that the nickel cations play the role of Lewis acid centers. Nkosi et al. [6] reported that the acidity is due to the hydrolysis of the $[Ni(H_2O)_6]^{2+}$ species (known as the Planck mechanism [25]). Mosqueda-Jiménez et al. have evaluated the concentration and the nature of acid sites of Ni-MOR by NH_3-TPD and IR spectroscopy [26]. Their results indicate the formation of additional Brønsted acid sites after Ni^{2+} ion exchange of NaMOR; moreover, for each Ni^{2+} ion incorporated two acid sites were formed. One of these sites results from the hydrolysis of the $Ni^{2+}Z^-$ complex and the other is associated with the $NiOH^+$ groups of the Ni^{2+} ($Ni^{2+} + H_2O \rightarrow [Ni(OH)]^+ + H^+$).

The nature of the Ni species in NiMSA samples was investigated by TPR measurements. For NiMSA20 catalyst (Fig. 4), as well as for all nickel-exchanged MSA samples, the TPR profile showed only a band located between 700 and 900 °C, which we attribute to the hard reduction of Ni^{2+} to Ni^0.

To confirm this assertion, the reduced sample was treated in the same reactor, in air flow, at 800 °C for 5 h resulting in the generation of Ni-oxide species ($Ni^0 + \frac{1}{2}O_2 \rightarrow NiO$). The NiO-MSA20 sample was then cooled at 25 °C and a new TPR measurement was performed in the same way as above (see Experimental section). A narrow peak centered at 350 °C was obtained for the reduction of NiO species (Fig. 4). These TPR measurements clearly indicate the absence of bulk nickel oxide in our NiMSA catalysts. The only cationic Ni^{2+} species present in mesoporous materials strongly interact with the support making very difficult their reduction. This agrees with the results recently reported by Lewandowska et al. [27].

3.2. Catalytic activity

3.2.1. Role of nickel sites

In order to spotlight the role of nickel in the oligomerization of ethylene, separate experiments using NaMSA30, HMSA30, and NiMSA30 as catalysts were performed. Both Na^+ and H^+ forms of Ni free Al-MCM-41 were completely inactive for ethylene oligomerization at 150 °C, 3.5 MPa, in *n*-heptane as solvent, whereas NiMSA sample showed a high activity (41.4 $g_{ethylene}$ converted/(g_{cat} h)) under these conditions. These results indicate that the nickel sites play an indispensable role in the ethylene oligomerization. Other preliminary tests with NiMSA catalysts showed that the ethylene oligomerization is completely inhibited by the presence of oxygen in the reactor.

3.2.2. Selection of the solvent

It is known that the solvent plays a very important role in the liquid-phase catalytic reactions. Therefore, the effect of various common solvents on the catalytic oligomerization of ethylene was investigated. The reaction was carried out at 150 °C and 3.5 MPa, using NiMSA30 as catalyst. The performances of various solvents, expressed in terms of

Table 2
Solvent effect in ethylene oligomerization over NiMSA30

Entry	Solvent	Activity (g/(g h)[a])
1	*n*-Heptane	41.4
2	Toluene	28.7
3	Cyclohexane	26.3
4	*iso*-Octane	8.2
5	*n*-Decane	5.5

[a] $g_{\text{oligomers}}/(g_{\text{cat}}\,h)$.

oligomers quantity per unit mass of catalyst and time, are listed in Table 2.

These results clearly indicate the favorable effect of *n*-heptane as solvent in the ethylene oligomerization. The lower conversions of ethene are probably due to its low solubility in some tested solvents. Moreover, the analysis of the oligomeric products indicated that toluene and *n*-decane were strongly involved in parallel reactions such as alkylation and isomerization, respectively. Next, the effectiveness of various catalysts was investigated in *n*-heptane as solvent.

3.2.3. *Effect of temperature and ethylene pressure*

The effect of the reaction temperature was investigated on NiMSA10 and NiMSA50 catalysts. Oligomerization runs were performed in *n*-heptane, at 3.5 MPa, with reaction temperatures selected between 50 and 200 °C. As can be seen from Fig. 5, in both cases the catalytic activity goes through a maximum for a temperature of about 150 °C.

The pronounced fall in conversion at a temperature above 150 °C can be attributed to the fast catalyst deactivation at higher temperatures or/and to the instability of the surface organometallic species (responsible for oligomerization), as previously reported [11]. We note that similar volcano-type curves were observed for ethylene and propene oligomerization in a fixed-bed flow reactor over nickel-exchanged amorphous silica–alumina catalysts [28]. A strong effect of the reaction temperature on the oligomers distribution was also observed over our catalysts, but this aspect will be discussed in the next section.

NiMSA30 catalyst has been chosen for testing the effect of the pressure on the activity in the ethylene oligomerization. As expected, the role of the pressure in three-phase gas–liquid–solid reaction system was very important (Fig. 6). Thus, the catalytic activity increased linearly by increasing ethylene pressure from 2 to 5 MPa. We consider that this behavior is principally due to ethylene solubility dependence on pressure. For technical reasons further experiments will be performed at 3.5 MPa.

3.2.4. *Influence of the acid site concentration*

The catalytic properties of NiMSA materials with different acid sites concentration and close Ni-loading (see Table 1) were evaluated for the same reaction conditions 150 °C, 3.5 MPa, in *n*-heptane as solvent. As shown in Fig. 7 the acid site density has a great importance in controlling the activity of tested catalysts. The amount of oligomers

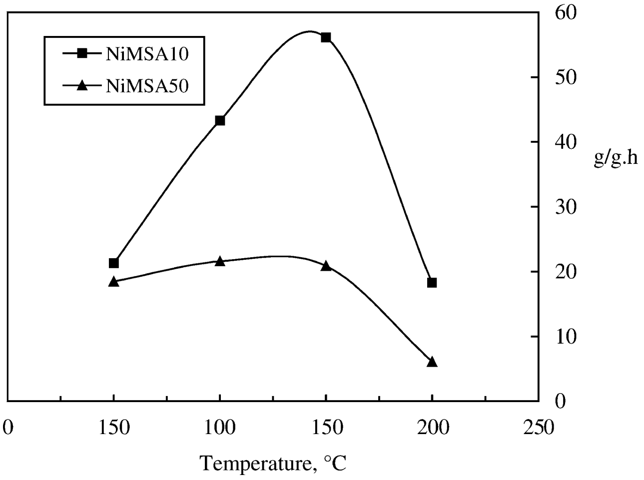

Fig. 5. Effect of the reaction temperature on the amount of oligomers (60 min, *n*-heptane, 3.5 MPa).

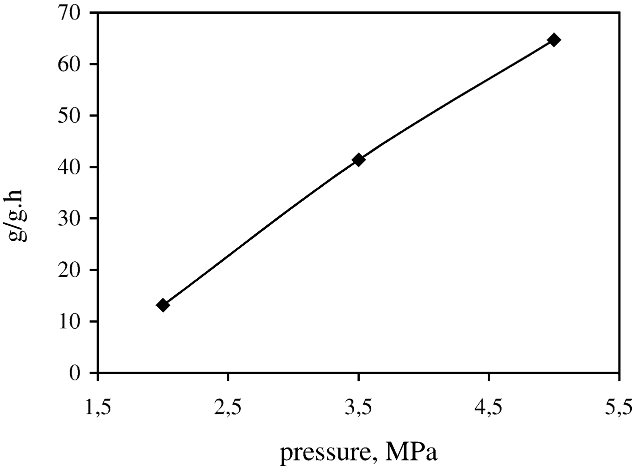

Fig. 6. Effect of the ethylene pressure on the amount of oligomers (60 min, *n*-heptane, 150 °C, catalyst NiMSA30).

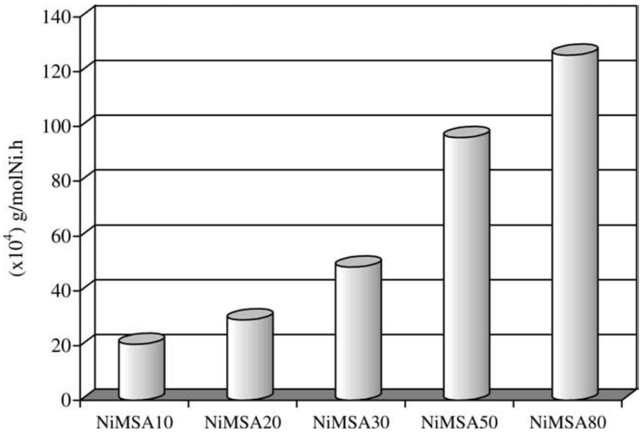

Fig. 7. Catalytic activity of NiMSA samples (in *n*-heptane, after 60 min, at 150 °C and 3.5 MPa).

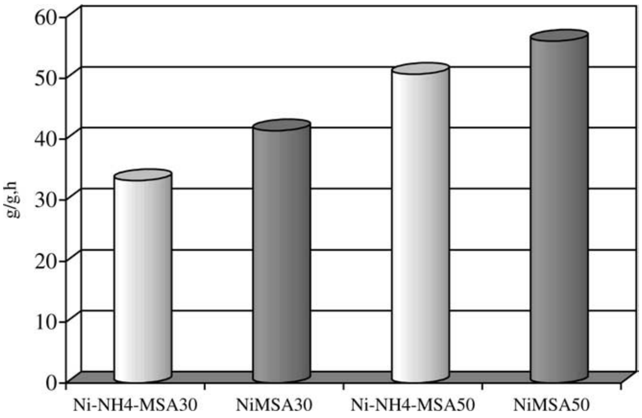

Fig. 8. Effect of the acidic properties on the catalytic activity (n-heptane, 60 min, 150 °C, 3.5 MPa).

($g_{\mathrm{oligomers}}$ per mole of Ni and hour) strongly increases when the acidic site concentration decreases from 0.72 mmol $NH_3/g_{NiMSA10}$ to 0.3 mmol $NH_3/g_{NiMSA80}$.

On the basis of this trend, two questions concerning the impact of the acid properties of oligomerization catalysts could be formulated: (i) Is the presence of acid sites (still) required? (ii) Why is a high density of acid sites so unfavorable to the ethylene conversion?

To clarify the role of acid sites, the ethylene oligomerization was carried out in presence of a Ni–NH_4-MSA catalyst, which is the noncalcined Ni-MSA sample (see experimental part). We can consider that most of the Brønsted acid sites are neutralized in the Ni–NH_4-MSA sample. As shown in Fig. 8, for both 30 and 50 Si/Al ratios, the activity of the NH_4-form catalyst was lower compared to H-form catalysts.

It appears from these results that a too low acidity is detrimental for the catalytic activity and therefore we consider that both nickel and acidic sites are required for the activation of ethylene. Some earlier reports concerning the effect of acidity support this assertion. Thus, Davydov et al. [29] showed the essential role played by the acid sites, which are required to promote the Ni^{2+}/Ni^{+} redox cycle and to stabilize the Ni^{+} ions involved in the ethylene oligomerization. In general, there is agreement that the isolated Ni^{+} species are the active metal sites for this reaction [4,12,29]. Moreover, Ng et al. suggested that the Ni^{+}–H^{+} couple is involved in the oligomerization mechanism of ethylene [7]. It was also previously reported that the ethylene oligomerization activity of the nickel-exchanged silica–alumina is proportional to the acid strength of the surface [7,30]. Though the present study points to a positive role of acidity, our data do not allow more precise conclusions regarding the implication of acid sites in the oligomerization reaction mechanism of ethylene to be drawn.

As concerns the ill-fated effect of the high density of acid sites on catalytic performances (Fig. 7), a possible explanation could be formulated on the basis of the results presented in Fig. 9. In this figure, the amounts of oligomers vs reaction time for three samples with very different acid site concentration were plotted. For all samples, as the reaction proceeded, the catalytic activity gradually decreased. As can be seen from these results, the most acid NiMSA10 catalyst suffered severe deactivation after only 15–20 min of reaction (when the amount of oligomers reaches a plateau). On the contrary, a remarkable stability (the oligomers quantity increases constantly with reaction time) was observed in the case of the less acid NiMSA80 sample. The performance of the moderately acid NiMSA30 places this sample between the other two.

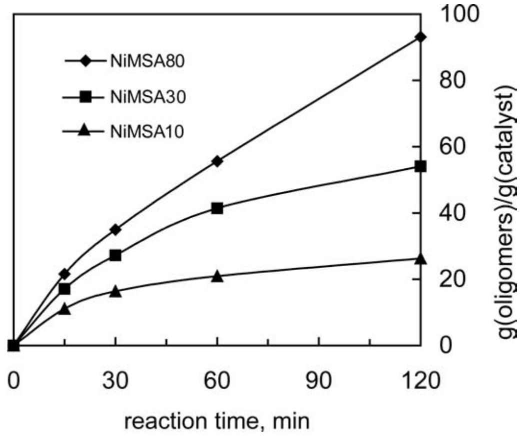

Fig. 9. Evolution of catalytic activity along reaction time during C_2H_4 oligomerization in n-heptane, at 150 °C and 3.5 MPa.

It is of importance to study the state of catalysts after performing the reaction of the oligomerization of ethylene. Thus, the spent catalysts were characterized using several methods, such as N_2 sorption, TPD, TPR, and TGA/DTA. No obvious change was observed between N_2 isotherms and TPR profiles of fresh and spent catalysts, indicating that both textural properties of catalyst and nickel state did not change during the oligomerization reaction. Moreover, no nickel leaching was confirmed by elemental analysis. However, the TPD measurements revealed a certain diminution of the acid site concentration of spent catalysts. We also observed that the amount of organic compounds deposition over used catalysts (evaluated by TGA) increased with increasing acid site concentration of NiMSA catalysts.

According to these results we can suppose that a high acid/nickel ion sites ratio results in rapid surface deactivation of Ni-containing materials due to acid-catalyzed reactions, which are responsible for the formation of strong adsorbed long-chain oligomers. Consequently, only a carefully selected acid sites density has a beneficial influence on the stability of NiMSA catalyst and implicitly on the oligomerization activity.

3.2.5. *Effect of pore size of catalyst*

The catalytic activity of several NiMSA samples with 35–40 Å pore size were investigated here above. In order to check the effect of mesopore diameter, we have examined the ethylene oligomerization over two NiMSA30 samples with 37 and 86 Å pore sizes. According to Fig. 10, there are obvious differences between the catalytic performances of

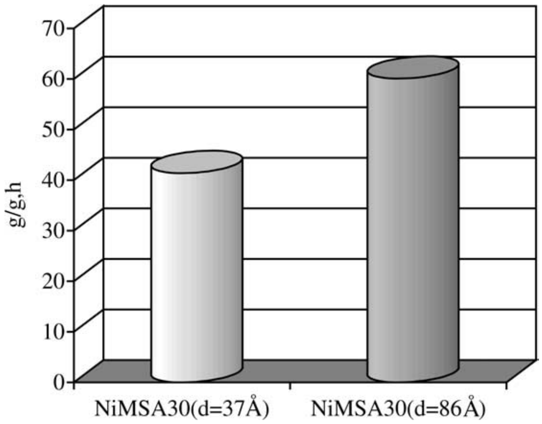

Fig. 10. Effect of the pore size of NiMSA30 catalyst (*n*-heptane, 60 min, 150 °C, 3.5 MPa).

two samples which possess the same Si/Al ratio (30), acidity (0.45 mmol NH_3/g), and Ni content (0.5 wt%). It can be concluded from this fact that the presence in NiMSA30 ($d = 86$ Å) catalyst of mesopores with 86 Å diameter could be the most important cause for its higher catalytic activity. In fact, the larger pores are beneficial to the diffusion of branched-chain higher oligomers, and thus result in lower deactivation rate.

3.3. Product distribution

It was previously reported that in the presence of strongly acidic nickel-exchanged zeolites a broad range of hydrocarbons was formed by ethylene oligomerization, as well as by cracking, isomerization, and hydrogenation parallel reactions [5,6]. Under the present experimental conditions, over NiMSA catalysts, the ethylene oligomerization was highly selective, resulting almost exclusively in C_4–C_{12} olefins with an even number of carbon atoms. Traces of C_{14+} unsaturated hydrocarbons were identified in the oligomeric products. No alkanes, aromatics, and odd number alkenes were present, indicating that acid-catalyzed cracking or hydrogen transfer reactions are not occurring to a significant level.

The selectivity toward different hydrocarbon groups depended on both acid properties of catalyst and operation conditions. From Fig. 11, when the C_n distribution was plotted against the acid sites concentration of NiMSA samples, it can be observed that the main oligomerization product was C_4 olefins. A large amount of C_6 olefins (35 mass%) was also obtained for the catalyst with the lowest acid site concentration. The increase in acid site density results in decrease of C_4–C_6/C_{8+} ratio.

Moreover, in additional experiments, we found that the amount of C_{8+} olefins obtained over Ni-MSA30 (34.2 mass%) was much higher than over Ni–NH_4-MSA30 (13.4 mass%). These changes in the product distribution suggest that a higher acid sites concentration is favorable of further oligomerization of the initial C_4 and C_6 olefins, resulting in C_{8+} hydrocarbons formation.

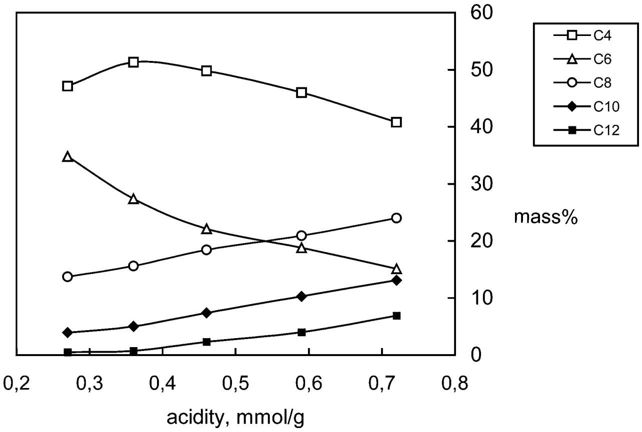

Fig. 11. Product distribution per carbon atom number vs acidity; 150 °C, 3.5 MPa, *n*-heptane.

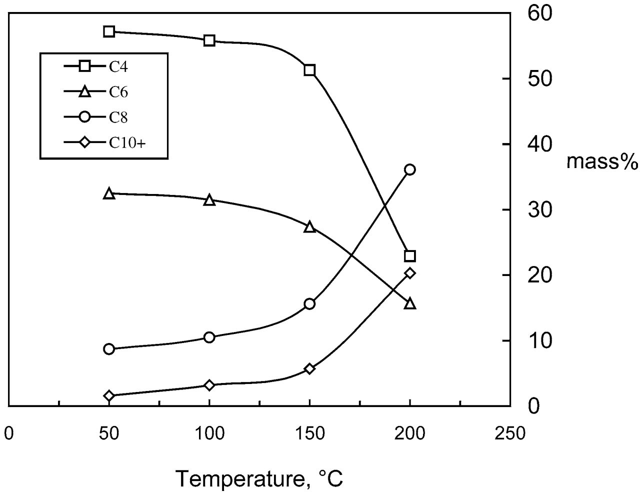

Fig. 12. Effect of reaction temperature on product distribution; catalyst NiMSA50, $p = 3.5$ MPa.

The oligomers distribution was strongly affected by the reaction temperature and ethylene pressure. Thus, for temperatures less than 150 °C the oligomerization was mainly directed toward the formation of C_4 and C_6 olefins (Fig. 12). On the contrary, at the high temperatures, acid-catalyzed site reactions (hetero-oligomerization), to which the primary product alkenes are more susceptible than ethylene itself, play an important role. Thus, the high-temperature region is characterized by large amounts of C_8 and C_{10+} hydrocarbons.

An increase in the average molecular mass of oligomers was also observed with an increase in ethylene pressure. We found that over NiMSA50 catalyst, at 150 °C, the amount of C_{8+} hydrocarbons increased from 21.3 mass% at 3.5 MPa to 32 mass% at 5.0 MPa. We note that the product distribution did not significantly vary with the pore size of the mesoporous catalysts (at 150 °C and 3.5 MPa).

It is interesting to analyze the distribution of isomers for each C_n olefin. Looking at the composition of butenes shown in Fig. 13, it is evident that for all tested catalysts 2-butene

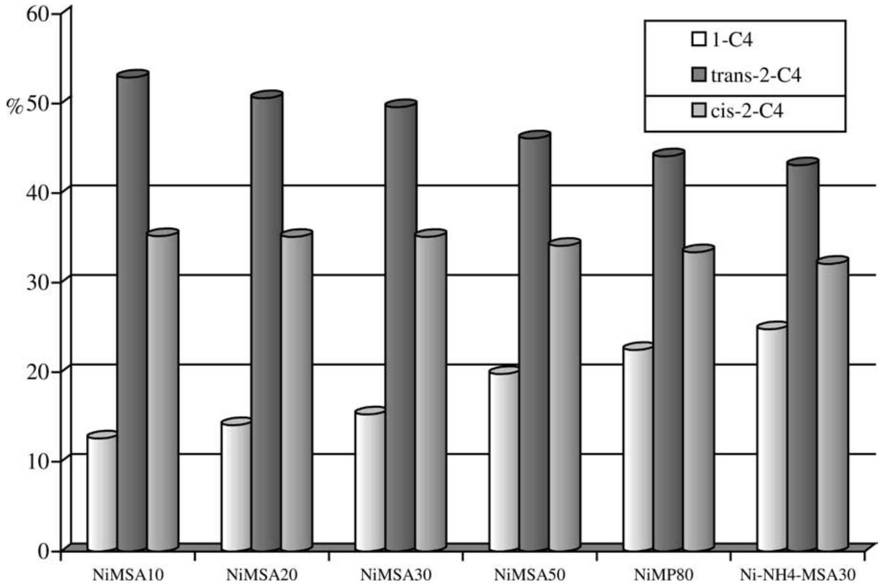

Fig. 13. C_4 olefins distribution; 150 °C, 3.5 MPa, *n*-heptane.

predominates as compared with 1-butene. Only traces of *i*-butene were detected among C_4 isomers.

Fig. 13 clearly indicates that C_4 olefin distribution is dependent on the acidic properties of the catalyst. Higher Si/Al ratio (lower acid site density) results in a higher selectivity for 1-butene. The less acidic Ni–NH_4-MSA30 sample also favored the formation of a high amount of 1-butene. The reaction temperature plays again a significant role in determining the distribution of C_4 hydrocarbons (Fig. 14). It is evident that the selectivity toward 1-butene sharply decreases with increasing temperature. These results suggest that 1-butene is among the initial products of ethylene oligomerization and that its acid-catalyzed isomerization to 2-butene becomes prominent even at mild temperature.

With regards the C_6 isomers distribution, the results obtained over NiMSA samples (Table 3) show that the linear isomers and especially the hexene-2 predominate as compared with other ethylene trimers. A maximum selectivity of 55.5% hexene-2 was obtained with the most acid catalyst NiMSA10.

It is noteworthy that the *trans*-hexene-2/*cis*-hexene-2 ratio was about 2.5 over all catalysts. Generaly, at 150 °C the

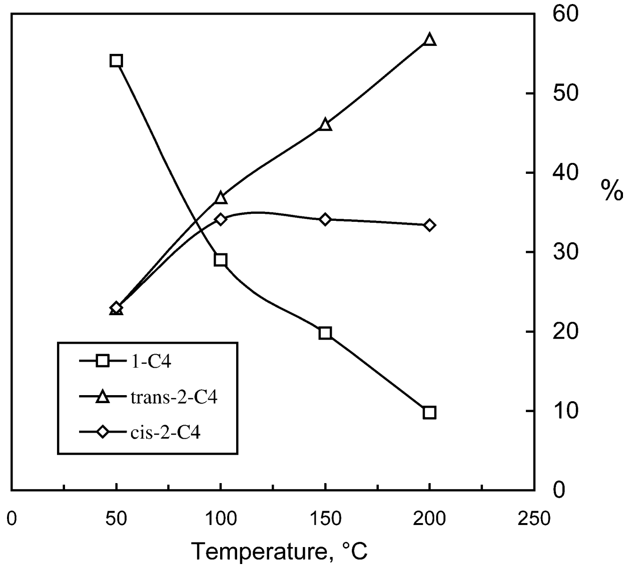

Fig. 14. Temperature effect on C_4 isomers distribution; catalyst NiMSA50, $p = 3.5$ MPa.

Table 3
C_6 olefins distribution; 150 °C, 3.5 MPa, *n*-heptane

Entry	Catalyst	Temperature (°C)	% 1-Hexene	2-Hexene	3-Hexene	Methyl-pentenes
1	NiMSA10	150	4.2	55.5	16	24.8
2	NiMSA20	150	4.2	50.7	15	26.9
3	NiMSA30	150	4.6	49.0	14.7	31.6
4	NiMSA50	150	5.6	44.9	13.8	35.6
5	NiMSA80	150	6.3	44.1	15.1	34.5
6	NiMSA50	50	19.4	41.8	17.1	21.7
7	NiMSA50	100	8.4	47.9	15.3	28.4
8	NiMSA50	200	4.3	46.1	13.2	35.5
9	NH_4MSA50	150	7.1	45.6	15.4	31.9

Table 4
Linear and branched C_6–C_{10} oligomers (LO = % linear olefins, BO = % branched olefins)

Catalyst	Temperature	C_6		C_8		C_{10}	
	(°C)	LO	BO	LO	BO	LO	BO
NiMSA10	150	75.2	24.8	9.7	90.3	2.0	98.0
NiMSA30	150	68.4	31.6	13.3	86.7	3.9	96.1
NiMSA50	150	64.4	35.6	22	78	8.9	91.1
NiMSA80	150	63.5	36.5	27.6	62.4	12.3	87.7
NiMSA50	50	78.3	21.7	34.4	65.6	15.9	84.1
NiMSA50	200	48.1	51.9	3.1	96.9	0.1	99.9

hexene-1 isomer concentration was 4–6%, but the proportion of this olefin increases up to 19.4% when the reaction temperature was 50 °C (Table 3, entries 4, 6, 7, and 8). These results suggest that hexene-1 could be the initial trimer product but the high rate of double-bound shift leads to the formation of thermodynamically stable internal alkene products. With respect to the composition of branched C_6 isomers, mainly the 3-methyl-C_5 chain structure was identified in the reaction products.

The estimation of the ratio between linear and branched products for the carbon number range C_6–C_{12} was obtained after hydrogenation of oligomers according to the method described by Heveling et al. [15]. The hydrogenation was performed in a batch reactor using a commercial Pd/C hydrogenation catalyst, at 100 °C and 1.5 MPa. A simplified chromatogram of saturated hydrocarbons is obtained and the n-alkanes can be easily identified.

According to Table 4, the C_6 oligomers are mainly linear isomers, and the amount of these trimers decreases with decreasing acid site concentration (from NiMSA10 to NiMSA80). A drastic decrease of the proportion of linear isomers was observed in the case of C_{8+} oligomers. This is a proof that the higher oligomers are mainly formed via acid-catalyzed reactions involving C_4 and C_6 primary olefins. It is known that this reaction type results in branched hydrocarbon formation. For all olefins, the isomers of higher linearity are favored by low temperatures, indicating a lower contribution of nonselective reactions under these conditions.

3.4. Reaction network

Based on the experimental results it is evident that several parallel and consecutive reactions involving both ethylene and primary oligomers may occur under our reaction conditions. The oligomerization network is governed by both the acidic properties of the catalyst and the reaction parameters. A possible reaction network for the ethylene transformation over Ni-MSA catalysts is given in Scheme 1.

The initial nickel-catalyzed reaction is the oligomerization of pure ethylene yielding 1-butene. We consider that the nickel cations also act as active sites for further oligomerization reactions (o) involving butene–ethylene and hexene–ethylene couples. Subsequent double bond isomerization (i) of primary C_4–C_8 olefins may be acid-catalyzed or it may also occurs on nickel sites. This reaction occurs even on weaker acid sites, particularly at mild and high temperature.

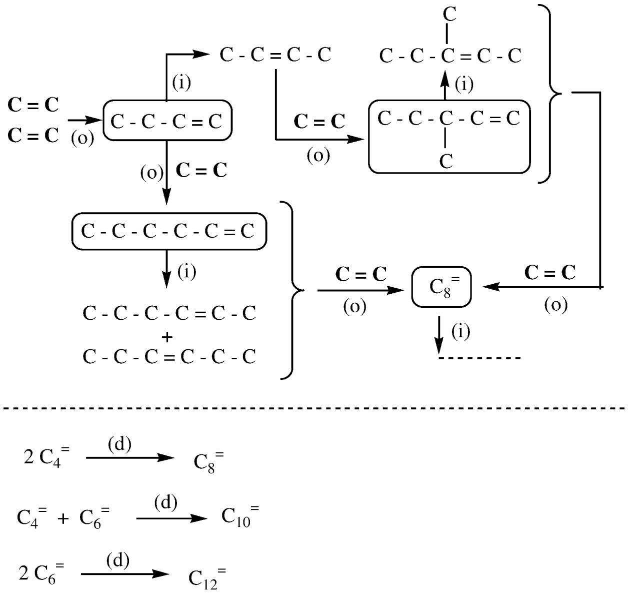

Scheme 1.

C_4 and C_6 olefins can also be consumed through dimerization reactions (d), which are essentially favored by a stronger acidity or/and a higher acid sites concentration. These reactions, occurring via a cationic mechanism, are responsible for the formation of strong adsorbed branched chain higher oligomers. The contribution of acid-catalyzed reactions becomes prominent at higher temperatures and pressures.

4. Conclusion

In this paper we have shown than Ni-exchanged well-mesostructured silica–alumina catalysts (Ni–AlMCM-41) reveal very interesting properties for ethylene oligomerization. The large and well-structured pores of the catalysts are very favorable for oligomerization process. The amounts of oligomers (20.5–63.2 g/(g_{cat} h)) formed with these catalysts were much higher than those reported previously [11] with Ni-exchanged amorphous silica–alumina, under closely related conditions. The reaction was highly selective, resulting almost exclusively in olefins with an even number of carbon atoms.

In agreement with literature data, we found that both nickel and acid sites are required for the activation of this reaction. Moreover, the acid density plays a significant role in determining the activity, stability, and selectivity. We have shown in this work that with Ni–AlMCM-41 catalysts, it is possible to achieve a desired balance between acid and nickel ion sites (by the proper choice of the Si/Al ratio and ion exchange level) so that high catalyst stabilities and high selectivities to suitable products can be achieved. These interesting catalytic performances were obtained under mild reaction conditions, in a slurry batch reactor.

In order to establish the kinetic parameters and the longer term behavior of Ni–AlMCM-41 catalysts, further investigations on the ethylene oligomerization, using a CSTR reactor, are in progress in our laboratory.

Acknowledgment

V. Hulea thanks CNRS for a research-associate position.

References

[1] A.M. Al-Jarallah, J.A. Anabtawi, A.A.B. Siddiqui, A.M. Aitani, A.W. Alsadoun, Catal. Today 14 (1992) 1.
[2] T. Yashima, Y. Ushida, M. Ebisawa, N. Hara, J. Catal. 36 (1975) 320.
[3] L. Bonneviot, D. Olivier, M. Che, J. Mol. Catal. 21 (1983) 415.
[4] J.V. Elev, B.N. Shelinov, V.B. Kazansky, J. Catal. 89 (1984) 470.
[5] J. Heveling, A. van der Beek, M. de Pender, Appl. Catal. 42 (1988) 325.
[6] B. Nkosi, F.T.T. Ng, G.L. Rempel, Appl. Catal. A 158 (1997) 225.
[7] F.T.T. Ng, D.C. Creaser, Appl. Catal. A 119 (1994) 327.
[8] L. Zhang, G. Wang, X. Bai, Stud. Surf. Sci. Catal. 28 (1986) 965.
[9] Q. Zhang, M. Kantcheva, I.G. Dalla Lana, Ind. Eng. Chem. Res. 36 (1997) 3433.
[10] Q. Zhang, I.G. Dalla Lana, Chem. Eng. Sci. 21/22 (1997) 4187.
[11] M.D. Heydenrych, C.P. Nicolaides, M.S. Scurrell, J. Catal. 197 (2001) 49.
[12] T. Cai, Catal. Today 51 (1999) 153.
[13] R.L. Espinoza, C.J. Korf, C.P. Nicolaides, R. Snel, Appl. Catal. 29 (1987) 175.
[14] R.L. Espinoza, C.P. Nicolaides, C.J. Korf, R. Snel, Appl. Catal. 31 (1987) 259.
[15] J. Heveling, C.P. Nicolaides, M.S. Scurrell, Appl. Catal. A 173 (1998) 1.
[16] C.P. Nicolaides, M.S. Scurrell, P.M. Semano, Appl. Catal. A 245 (2003) 45.
[17] L. Bonneviot, M. Che, K. Dyrek, R. Schollner, G. Wendt, J. Phys. Chem. 90 (1986) 2379.
[18] M. Kermarec, C. Lepetit, F.X. Cai, D. Olivier, J. Chem. Soc., Faraday Trans. I 85 (1989) 1991.
[19] T. Cai, D. Cao, Z. Song, L. Li, Appl. Catal. A 95 (1993) L1.
[20] J.S. Beck, J.C. Vartuli, W.J. Roth, M.E. Leonowicz, C.T. Kresge, K.D. Schmit, C.T.-W. Chu, D.H. Olson, E.W. Sheppared, S.B. McCullen, J.B. Higgins, J.L. Schlenker, J. Am. Chem. Soc. 114 (1992) 10834.
[21] M. Hartmann, A. Poppl, L. Kevan, J. Phys. Chem. 100 (1996) 9906.
[22] D. Desplantier-Giscard, A. Galarneau, F. Di Renzo, F. Fajula, Stud. Surf. Sci. Catal. 135 (2001) 06-P-27.
[23] K.S.W. Sing, D.H. Everett, R.A.W. Haul, L. Moscou, R.A. Pierotti, J. Rouquérol, T. Siemieniewska, Pure Appl. Chem. 57 (1985) 603.
[24] C. Minchev, S.A. Zubkov, V. Valtchev, V. Minkov, N. Micheva, V. Kanazirev, Appl. Catal. A 119 (1994) 195.
[25] C.S. Planck, in: Proceedings of Third International Congress Catalysis, Amsterdam, vol. 1, 1965, p. 727.
[26] B.I. Mosqueda-Jiménez, A. Jentys, K. Seshan, J.A. Lercher, Appl. Catal. B 46 (2003) 189.
[27] A. Lewandowska, S. Monteversdi, M. Bettahar, M. Ziolek, J. Mol. Catal. A 188 (2002) 85.
[28] J. Heveling, C.P. Nicolaides, M.S. Scurrell, Appl. Catal. A 248 (2003) 239.
[29] A.A. Davydov, M. Kantcheva, M.L. Chepotko, Catal. Lett. 83 (2002) 97.
[30] R.L. Espinoza, R. Snel, C.J. Korf, C.P. Nicolaides, Appl. Catal. 29 (1987) 295.